J Appl Physiol 117: 604–615, 2014.
First published July 31, 2014; doi:10.1152/japplphysiol.00174.2014.

Are running speeds maximized with simple-spring stance mechanics?

Kenneth P. Clark and Peter G. Weyand

Southern Methodist University, Locomotor Performance Laboratory, Department of Applied Physiology and Wellness, Dallas, Texas

Submitted 24 February 2014; accepted in final form 24 July 2014

Clark KP, Weyand PG. Are running speeds maximized with simple-spring stance mechanics?. *J Appl Physiol* 117: 604–615, 2014. First published July 31, 2014; doi:10.1152/japplphysiol.00174.2014.—Are the fastest running speeds achieved using the simple-spring stance mechanics predicted by the classic spring-mass model? We hypothesized that a passive, linear-spring model would not account for the running mechanics that maximize ground force application and speed. We tested this hypothesis by comparing patterns of ground force application across athletic specialization (competitive sprinters vs. athlete nonsprinters, $n = 7$ each) and running speed (top speeds vs. slower ones). Vertical ground reaction forces at 5.0 and 7.0 m/s, and individual top speeds ($n = 797$ total footfalls) were acquired while subjects ran on a custom, high-speed force treadmill. The goodness of fit between measured vertical force vs. time waveform patterns and the patterns predicted by the spring-mass model were assessed using the R^2 statistic (where an R^2 of 1.00 = perfect fit). As hypothesized, the force application patterns of the competitive sprinters deviated significantly more from the simple-spring pattern than those of the athlete, nonsprinters across the three test speeds ($R^2 < 0.85$ vs. $R^2 \geq 0.91$, respectively), and deviated most at top speed ($R^2 = 0.78 \pm 0.02$). Sprinters attained faster top speeds than nonsprinters (10.4 ± 0.3 vs. 8.7 ± 0.3 m/s) by applying greater vertical forces during the first half (2.65 ± 0.05 vs. 2.21 ± 0.05 body wt), but not the second half (1.71 ± 0.04 vs. 1.73 ± 0.04 body wt) of the stance phase. We conclude that a passive, simple-spring model has limited application to sprint running performance because the swiftest runners use an asymmetrical pattern of force application to maximize ground reaction forces and attain faster speeds.

sprinting performance; musculoskeletal mechanics; ground reaction forces; gait; spring-mass model

RUNNING SWIFTLY IS AN ATHLETIC attribute that has captivated the human imagination from prehistoric times through the present day. However, interest in running speed as an athletic phenomenon has probably never been greater than at present. A number of factors have heightened contemporary interest and focused it upon the determinants of how swiftly humans can run. These factors include the globalization and professionalization of athletics, the parallel emergence of a performance-training profession, advances in scientific and technical methods for enhancing performance, and record-breaking sprint running performances in recent international competitions. Yet despite interest, incentives, and intervention options that are arguably all without precedent, the scientific understanding of how the fastest human running speeds are achieved remains significantly incomplete.

At the whole-body level, the basic gait mechanics responsible for the swiftest human running speeds are well established. Contrary to intuition, fast and slow runners take essentially the same amount of time to reposition their limbs when sprinting at their different respective top speeds (36, 38). Hence, the time taken to reposition the limbs in the air is not a differentiating factor for human speed. Rather, the predominant mechanism by which faster runners attain swifter speeds is by applying greater forces in relation to body mass during shorter periods of foot-ground force application (36, 38). What factors enable swifter runners to apply greater mass-specific ground forces? At present, this answer is unknown. Moreover, the limited scientific information that is available offers two competing possibilities.

The first possibility is drawn from the classic view of steady-speed running mechanics. In this classic view, runners optimize force production, economy, and overall performance by using their legs in a spring-like manner during each contact period with the ground (13, 16, 31). During the first portion of the stance phase, the limb is compressed as the body is pulled downward by the force of gravity, storing strain energy in the elastic tissues of the leg. In the latter portion of the stance phase, this strain energy is released via elastic recoil that lifts and accelerates the body into the next step (30). The stance phase dynamics observed have been modeled as a lumped point-mass bouncing atop a massless leg spring (2, 4, 18, 19, 26, 32). This simple model makes the basic predictions illustrated in Fig. 1*A*: *1*) the ground reaction force vs. time waveform will take the shape of a half-sine wave, *2*) the displacement of the body's center of mass during the compression and rebound portions of the contact period will be symmetrical about body weight, and *3*) the peak force will occur at midstance when the center of mass reaches its lowest position. Despite its mechanical simplicity, the classic spring-mass model provides relatively accurate predictions of the vertical force vs. time waveforms observed at slow and intermediate running speeds.

The second possibility emerges from the more limited ground reaction force data that are available from humans running at faster speeds. These more limited data (3, 5, 10, 23, 25, 35, 37, 38) generally exhibit vertical ground reaction force vs. time waveforms that are asymmetrical and therefore not fully consistent with the simple, linear-spring pattern predicted by the spring-mass model. Indeed, the tendency toward asymmetry appears to be most pronounced in the ground reaction force waveforms from the fastest speeds (3, 10, 37, 38), which show an appreciably steeper rising vs. trailing edge and a force peak that occurs well before midstance (Fig. 1*B*, *Example 1*). The more asymmetrical pattern at faster speeds may result from greater impact-phase limb decelerations (14) that elevate the ground reaction forces in the early portion of the stance phase. This mechanism would enhance ground force application within the short contact periods available during sprint running (36, 38) and appears to be consistent with gait kinematics used by the fastest human sprinters (24).

Address for reprint requests and other correspondence: P. Weyand, Locomotor Performance Laboratory, Dept. of Applied Physiology and Wellness, Southern Methodist Univ., 5538 Dyer St., Dallas, TX 75206 (e-mail: pweyand@smu.edu).

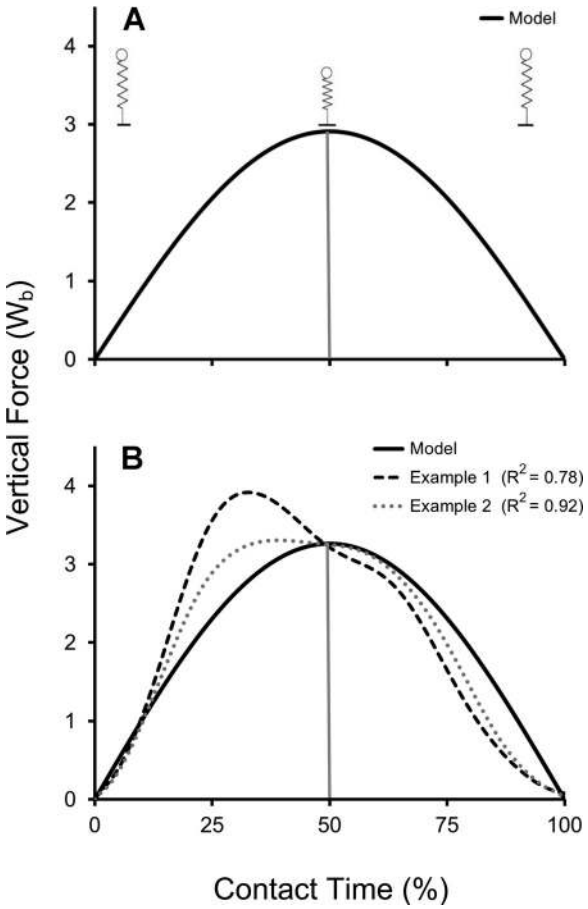

Fig. 1. A schematic illustration of the classic spring-mass model [modified with permission from (12)] during forward running and the half-sine waveform representing the vertical force produced by the mathematical expression of the model (*A*). The half-sine waveform representing the spring-mass model (solid black line) vs. two different example waveforms. *Example 1* (dashed black line) has relatively poor conformation to the model, whereas *Example 2* (dotted gray line) has relatively better conformation to the model (*B*). Ground reaction forces are presented in mass-specific form (i.e., after standardization to body weight) in all illustrations.

We undertook this study to evaluate whether or not the fastest human running speeds are achieved using simple, linear-spring stance mechanics. We did so using the vertical ground reaction force vs. time relationship predicted by the spring-mass model in Fig. 1*A* as a null standard for comparisons. We quantified conformation to, or deviation from, the pattern of ground force application predicted by the spring-mass model from the degree of overlap (i.e., goodness of fit, R^2) between modeled and measured waveforms as illustrated in Fig. 1*B*. Two experimental tools were used to test the idea that the fastest human running speeds are attained using an asymmetrical pattern of ground force application that deviates from the simple, linear spring predictions of the spring-mass model: *1*) athletic specialization and 2) running speed. In the first case, we hypothesized that patterns of ground force application of competitive sprinters would deviate more from spring-mass model predictions than those of athlete nonsprinters. In the second case, for subjects in both groups, we hypothesized that patterns of ground force application would deviate more from spring-mass model predictions at top speed vs. slower running speeds.

METHODS

Experimental Overview and Design

Spring model predictions. Per the methods outlined by Alexander et al. (2) and Robilliard and Wilson (32), half-sine wave formulations of the vertical ground reaction force waveforms predicted by the spring-mass model were determined from the runner's contact time (t_c), aerial time (t_{aer}), and step time ($t_{step} = t_c + t_{aer}$):

$$F(t)/W_b = \begin{cases} \left(\frac{\pi}{2}\right) \cdot \left(\frac{t_{step}}{t_c}\right) \cdot \sin\left(\pi \cdot \left(\frac{t}{t_c}\right)\right), & 0 \le t < t_c \\ 0, t_c \le t < t_{step} \end{cases} \quad (Eq.\ 1)$$

where $F(t)$ is the force at time t and W_b is the force of the body's weight. The peak mass-specific force, F_{peak}/W_b, occurs during ground contact t_c at time $t = t_c/2$:

$$\frac{F_{peak}}{W_b} = \left(\frac{\pi}{2}\right) \cdot \left(\frac{t_{step}}{t_c}\right) \quad (Eq.\ 2)$$

The degree of overlap between the measured vertical ground reaction force-time waveforms vs. those predicted by the spring-mass model was determined using the R^2 goodness of fit statistic and mass-specific force values as follows. First, differences between the force values measured during each millisecond and the overall waveform mean value were squared and summed to obtain an index of the total variation present within the waveform, or the total sum of squares [$SS_{total} = \Sigma(F/W_{b,\ measured} - F/W_{b,\ mean})^2$]. Next, the predictive error of the spring model was determined from the difference between the spring-modeled values (*Equations 1* and *2*) and measured force values also using the same sum of squares method [$SS_{error} = \Sigma(F/W_{b,\ measured} - F/W_{b,\ spring\ model})^2$]. Finally, the proportion of the total force waveform variation accounted for by the spring-mass model was then calculated using the R^2 statistic:

$$R^2 = 1 - \left(\frac{SS_{error}}{SS_{total}}\right) \quad (Eq.\ 3)$$

Accordingly, our spring-model goodness of fit R^2 values have a theoretical maximum 1.00 (where $R^2 = 1.00$ is exact agreement with the spring model). In practice, and on the basis of prior literature (14), we expected patterns that were relatively well predicted by the model to have R^2 agreement values $\geq$0.90 and patterns that were predicted relative poorly to have agreement values $<$0.90. This somewhat subjective threshold was identified simply to facilitate goodness-of-fit interpretations. The example waveforms appearing in Fig. 1*B* provide a frame of reference between the degree of waveform overlap with the spring-model and corresponding numeric R^2 values. In accordance with our respective hypotheses, we predicted that: *1*) the R^2 values for competitive sprinters would be significantly lower than those of athlete nonsprinters, and *2*) the R^2 values at top speed would be significantly lower than those at slower running speeds for the subjects in both groups.

In addition to the relative values provided by our R^2 spring-model goodness of fit index, we also quantified the agreement between measured patterns of ground force application and the spring model-predicted patterns in the units of force most relevant to sprinting performance (F/W_b). We did so using the root mean square error (RMSE) statistic as follows:

$$RMSE = \sqrt{\left(\frac{SS_{error}}{n}\right)} \quad (Eq.\ 4)$$

where n equals the number of observations. Accordingly, larger RMSE values will result from patterns of ground force application that deviate more from the spring-mass model, and vice versa. Hence, the RMSE can be here conceptualized as an index of force disagree-

ment between the measured force waveforms vs. those predicted by the spring-mass model expressed in force units of the body's weight. Thus for this second statistic, we predicted RMSE values would be: *1*) significantly greater for competitive sprinters vs. athlete nonsprinters, and *2*) significantly greater at top speed vs. slower speeds for the subjects in both groups.

We analyzed only the vertical component of the ground force because previous work (10, 36, 38) has directly linked stance-average, mass-specific vertical ground reaction forces to the sprinting speeds attained:

$$\text{Speed} = \left(\frac{F_{\text{avg}}}{W_b}\right) \cdot L_c \cdot Freq_{\text{step}} \qquad (Eq.\ 5)$$

where speed is the body's forward running velocity, F_{avg}/W_b is the stance-averaged vertical force applied to the running surface in units of the body's weight, L_c is the length of contact, or forward distance the body travels during the foot-ground contact period, and $Freq_{\text{step}}$ is $1/(t_{\text{step}})$. The equation has been shown to be accurate within 3.0% or less during steady-speed running (38). Because we used a simple vertical spring-mass model rather than a planar model for hypothesis testing, horizontal ground reaction forces were not included in the analysis.

Design and data acquisition strategies. For the competitive sprinter group, we recruited only track athletes who specialized in the 100- and 200-meter events and who had intercollegiate track and field experience or the equivalent. For the athlete nonsprinter group, we recruited athletes who regularly ran at high speeds for their sport specialization, but who were not competitive sprinters. In both groups, we recruited and enrolled only those athletes with midfoot and forefoot strike patterns because the fast subjects we were seeking to enroll do not heel strike when running at high speeds.

We maximized ground reaction force data quality and quantity by conducting tests on a high-speed force treadmill capable of acquiring data from a large number of consecutive footfalls at precisely controlled speeds. Acquiring equivalently robust data for the purpose of quantifying patterns of foot-ground force application using in-ground force plates would be difficult, or perhaps impossible, given that overground conditions greatly limit the number of footfalls acquired, and substantially increase the variability present in both running speeds and foot-strike patterns. For athletic subjects running on a treadmill vs. overground, prior studies have demonstrated a close correspondence between sprint running performances (9), sprinting kinematics (20), and patterns of ground force application at speeds at which comparative data are available (22, 29).

Although we acquired data from many speeds, we used the ground reaction force data from only three of these for hypothesis testing: 5 m/s, 7 m/s, and individual top speed.

Subjects and Participation

A total of 14 subjects (8 men, 6 women) volunteered and provided written, informed consent in accordance with the requirements of the local institutional review board. All subjects were between 19 and 31 yr of age and regularly active at the time of the testing. The compositions of the competitive sprinter group (age 23.9 ± 1.6 yr, height 1.72 ± 0.03 m, mass 73.8 ± 4.3 kg) and the athlete nonsprinter group (age 21.7 ± 1.5 yr, height 1.77 ± 0.03 m, mass 75.8 ± 4.6 kg) were gender balanced; both included four men and three women. Subjects ranged in athletic experience from intercollegiate team-sport athletes to professional, world-class track athletes. In the athlete, nonsprinter group, all seven subjects had intercollegiate athletic experience. In the competitive sprinter group, six of the seven subjects had intercollegiate track and field experience, five had international experience, and four had participated in both the Olympics and Track and Field World Championships. Physical characteristics and athletic specializations of all participants appear in Table 1. Also provided are the 100- and 200-m personal records of the competitive sprinters.

Measurements

Top speed. Participants were habituated to running on a custom, high-speed force treadmill during one or more familiarization sessions before undergoing top speed testing. For all trials, subjects were fastened into a safety harness attached to an overhead suspension that would support them above the treadmill belt in the event of a fall. The harness and ceiling suspension had sufficient slack to not impede the subjects' natural running mechanics. A progressive, discontinuous treadmill protocol similar to that described by Weyand et al. (36) was administered to determine each subject's top speed. The protocol began at speeds of 2.5 or 3.0 m/s and typically increased in 1.0 m/s increments for each trial at slower speeds and 0.2–0.5 m/s at faster speeds. Trial speeds were progressively increased until a speed was reached at which the subject could not complete eight consecutive steps without backward movement exceeding 0.2 m on the treadmill. Subjects typically made two to three unsuccessful attempts at the failure speed before the test was terminated. The top speed successfully completed was within 0.3 m/s of the failure speed for all subjects. For each trial, subjects straddled the treadmill belt as it was increased to the desired trial speed. Handrails on the sides of the treadmill were set at waist-height and aided subjects in their transition onto the moving belt. Once the treadmill belt had increased to the selected speed, subjects transitioned onto the belt by taking several steps before releasing the handrails. Data acquisition was not initiated until the subject had released the rails. There was no limit on the number of handrail-assisted steps the subjects could complete during their transition onto the belt. Trials at speeds slower than 5 m/s typically lasted 10 to 20 s, whereas trials at speeds faster than 5 m/s

Table 1. *Physical and descriptive characteristics of subjects*

Group	Sex	Age, yr	Height, m	Mass, kg	Sport	100-m PR, s	200-m PR, s
Sprinter	Male	28	1.85	91.6	Track and Field	9.96	20.57
Sprinter	Male	23	1.78	83.4	Track and Field	10.06	20.29
Sprinter	Male	20	1.74	74.4	Track and Field	10.26	21.10
Sprinter	Male	19	1.70	71.8	Track and Field	10.80	22.20
Sprinter	Female	23	1.70	61.8	Track and Field	11.12	22.29
Sprinter	Female	31	1.70	74.1	Track and Field	11.04	22.33
Sprinter	Female	23	1.60	59.4	Track and Field	11.52	24.04
Nonsprinter	Male	23	1.95	101.5	NCAA varsity football		
Nonsprinter	Male	19	1.74	72.7	NCAA club lacrosse		
Nonsprinter	Male	30	1.74	74.6	Former NCAA varsity soccer		
Nonsprinter	Male	20	1.79	78.4	Intercollegiate distance runner		
Nonsprinter	Female	19	1.76	72.6	Intercollegiate varsity soccer		
Nonsprinter	Female	20	1.70	64.4	Intercollegiate varsity soccer		
Nonsprinter	Female	21	1.74	66.3	Intercollegiate varsity soccer		

typically lasted less than 5 s. Subjects were instructed to take full recovery between trials. They typically took 1–2 min between slow and intermediate speed trials, and 1–10 min between faster speeds trials. To reduce the risk of injury or muscle soreness, testing was terminated before top speed was attained if the subjects reported muscle or joint discomfort.

Treadmill force data. Ground reaction force data were acquired at 1,000 Hz from a high-speed, three-axis, force treadmill (AMTI, Watertown, MA). The treadmill uses a Baldor BSM100C-4ATSAA custom high-speed servo motor and a Baldor SD23H2A22-E stock servo controller, and is capable of speeds of >20 m/s. The custom embedded force plate has a length of 198 cm and a width of 68 cm, and interfaces with an AMTI DigiAmp amplifier running NetForce software. The force data were postfiltered using a low-pass, fourth-order, zero-phase-shift Butterworth filter with a cutoff frequency of 25 Hz (39).

Stride timing, length, and center of mass motion variables were determined as follows. For each footfall, contact times were determined from the time the vertical force signal exceeded a threshold of 40 N. Aerial times were determined from the time elapsing between the end of one period of foot-ground contact and the beginning of the next. Step times were determined from the time elapsing during consecutive foot-ground contact and aerial times. Step frequencies were determined from the inverse of step times. Limb repositioning, or swing times, were determined from the time a given foot was not in contact with the running surface between consecutive steps. Contact lengths were determined by multiplying the time of foot-ground contact by the speed of the trial. Trial speeds were determined from the average belt velocity over time. The vertical displacement of the center of mass during ground contact period was determined by double integration of the vertical force waveforms following the procedures described by Cavagna (12).

Force data acquired. Individual subjects completed 12–20 treadmill trials during their top speed tests to failure. The number of consecutive footfalls from which force waveforms were acquired during these tests was generally greater for the slower, less demanding trials. For example, we typically acquired >20 consecutive footfalls for slow and intermediate speeds, 10–20 at moderately fast speeds, and 8–12 during top-speed and near top-speed trials.

The number of footfalls acquired at the subset of three speeds used for formal statistical testing purposes reflect the general pattern of acquiring fewer footfalls at faster speeds. For the competitive sprint and athlete nonsprint subjects, the average number of footfalls acquired at the three hypothesis test speeds were as follows: 31 and 28 at 5.0 m/s, 23 and 13 at 7.0 m/s, and 10 and 9 at top speed, respectively. The number of force waveforms acquired from the three selected speeds used for statistical testing purposes was 797. The total number of footfalls acquired from all subjects at all speeds was >3,000.

For illustrative purposes, ensemble-averaged waveforms were determined for individual subjects and the two subject groups at all of the trial speeds completed including the top sprinting speed. For individual subjects at each speed of interest, ensemble-averaged waveforms were generated by averaging the force from each millisecond of the stance period for all of the waveforms acquired. At those speeds completed by all seven subjects of the respective groups, the seven individual ensemble-averaged waveforms were combined to form ensemble-averages for each of the respective groups. These group force–time waveforms were compiled by standardizing the vertical force values to units of the body's weight and time values to the percentage of the total stance contact time. Neither the individual nor group ensemble averages were used for formal hypothesis testing purposes.

To provide a supplementary assessment of waveform shape characteristics, we also performed a basic Fourier analysis similar to that described by Alexander and Jayes (1), and which appears in the APPENDIX.

Statistics

Both hypothesis tests were evaluated using a two-factor ANOVA (group × speed) that analyzed the mean goodness of fit (R^2 values) between spring-model predicted ground reaction force waveforms and those directly measured from our subjects. Secondary tests of the same hypotheses were conducted using the RMSE statistic. For both force application hypothesis test one (group effect) and test two (speed effect), the a priori thresholds for significance were set at $\alpha = 0.05$. Homogeneity of variance was tested using the Fligner-Killeen test.

Percentage differences between group means for all variables were calculated as: {(larger − smaller)/[(larger + smaller)/2]} × 100. For stance-averaged vertical forces, mean percentage differences were calculated after subtracting a baseline value equal to 1.0 W_b for running at zero speed, or standing.

RESULTS

Top Speeds and Stance-Averaged Vertical Forces

Group means (±SE) for top speeds, stance-averaged vertical forces, contact times, aerial times, swing times, and contact lengths at top speed appear in Table 2. The table includes the overall group means for the competitive sprinters and athlete nonsprinters as well as the within-group means for the men and women. For the overall means, the between-group differences in two variables, top speed ($\Delta = 1.64$ m/s) and stance-averaged vertical forces ($\Delta = 0.21\ W_b$), when expressed on a percentage basis (top speed $\Delta = 17.2\%$; stance-average vertical force $\Delta = 19.2\%$), were nearly identical. The similar percentage differences in top speed and stance-averaged force means variables across the groups resulted from the lack of variation in mean contact lengths and step frequencies (Equation 5).

When considered by sex, between-group differences in top speeds and stance-averaged vertical forces were both slightly larger for women vs. men (top speed $\Delta = 1.76$ vs. 1.56 m/s;

Table 2. *Top-speed gait mechanics*

Group	Top Speed, m/s	F_{avg}, W_b	L_c, m	t_c, s	t_{aer}, s	T_{sw}, s	$Freq_{step}$, s^{-1}
Sprinter							
Males	10.84 ± 0.12	2.18 ± 0.02	1.10 ± 0.04	0.102 ± 0.004	0.114 ± 0.004	0.330 ± 0.010	4.65 ± 0.14
Females	9.73 ± 0.35	2.22 ± 0.06	0.96 ± 0.05	0.099 ± 0.002	0.118 ± 0.004	0.335 ± 0.006	4.61 ± 0.06
Average	10.36 ± 0.27	2.20 ± 0.03	1.04 ± 0.04	0.100 ± 0.002	0.116 ± 0.003	0.332 ± 0.006	4.63 ± 0.08
Nonsprinter							
Males	9.28 ± 0.17	2.01 ± 0.07	1.04 ± 0.06	0.112 ± 0.006	0.111 ± 0.006	0.334 ± 0.012	4.49 ± 0.14
Females	7.97 ± 0.19	1.95 ± 0.01	0.96 ± 0.02	0.121 ± 0.001	0.113 ± 0.005	0.346 ± 0.010	4.29 ± 0.10
Average	8.72 ± 0.29	1.99 ± 0.04	1.01 ± 0.03	0.116 ± 0.004	0.112 ± 0.004	0.340 ± 0.008	4.40 ± 0.09

Values are means ± SE. L_c, length of contact; t_c, runner's contact time; t_{aer}, runner's aerial time; t_{SW}, swing time; $Freq_{step}$, $1/(t_{step})$.

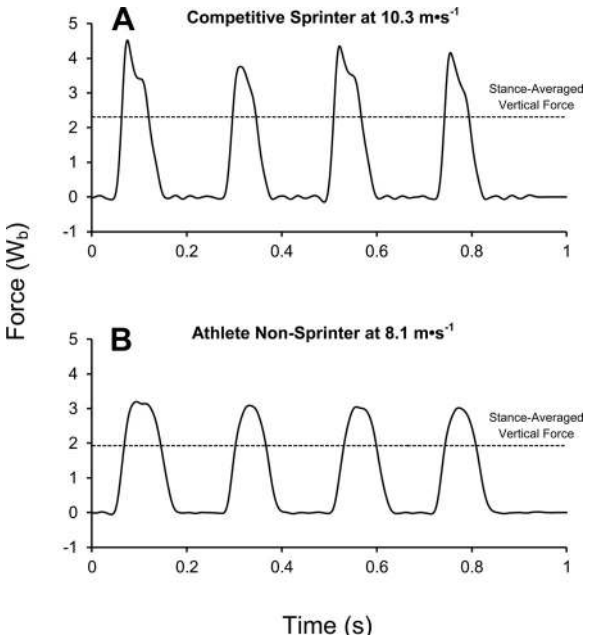

Fig. 2. Vertical ground reaction forces from four consecutive steps for a female competitive sprinter (*A*) and a female athlete nonsprinter (*B*) at their individual top speeds (10.3 and 8.1 m/s, respectively). The stance-averaged vertical forces applied during the respective trials are represented by the dashed horizontal lines. The competitive sprinter applies greater stance-averaged and peak vertical forces during briefer contact phases than the athlete nonsprinter.

stance-averaged vertical force $\Delta = 0.27$ vs. 0.17 W_b). Because neither step frequencies nor stance-averaged vertical forces varied appreciably by gender, the top speed differences between male and female subjects resulted largely from differences in contact lengths. The latter were 10.8% shorter for the overall female vs. male mean (female vs. male ΔL_c sprinters = 13.6%, athlete nonsprinters = 8.0%).

Patterns of Ground Force Application as a Function of Running Speed

Ground force application data from the same two female subjects, one sprinter and one athlete nonsprinter, appear in Figs. 2 through 4 to allow the relationships between original force waveforms (Fig. 2), stance-averaged vertical forces (Fig. 3), and patterns of ground force application (Fig. 4) to be fully illustrated. The step-by-step, ground reaction force waveforms from the respective top-speed trials of these athletes (Fig. 2, *A* and *B*, respectively) were greater in magnitude and briefer in duration for the competitive sprinter vs. the athlete nonsprinter.

The mass-specific, stance-averaged vertical forces for both athletes (Fig. 3, *A* and *B*) increased in a largely linear fashion with speed, from a jog of 3.0 m/s through top speed, with values for the sprinter being 0.2 W_b greater across common speeds. Ensemble-averaged patterns of ground force application for the respective athletes at the same trial speeds (Fig. 4, *A* and *B*) illustrate that both athletes had relatively symmetrical waveforms at the slowest speed of 3.0 m/s. With increases in speed above 3.0 m/s, patterns of ground force application by the sprinter became progressively less symmetrical. The corresponding waveforms for the athlete nonsprinter were relatively symmetrical across all speeds, including her top sprinting speed.

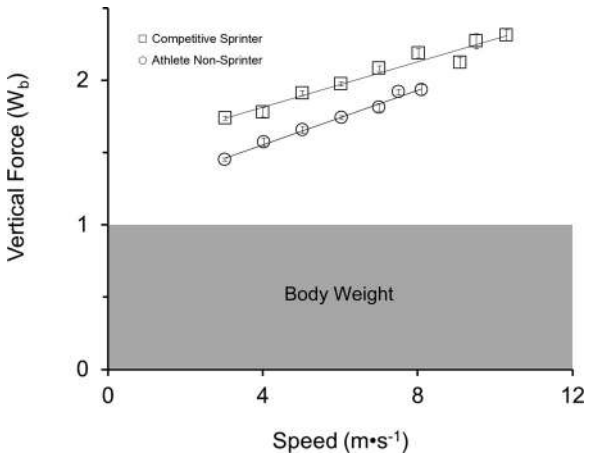

Fig. 3. Stance-averaged, vertical force (mean ± SE) vs. running speed for the same female competitive sprinter (squares) and female athlete nonsprinter (circles) whose data appear in Fig. 2. For both subjects, stance-averaged vertical forces increased across the range of speeds (linear best fits illustrated). The competitive sprinter applied greater forces at equal speeds and top speed.

Patterns of Ground Force Application vs. the Spring-Mass Model Predictions

Ensemble-averaged patterns of ground force application at 5.0 m/s, 7.0 m/s, and top speed, as well as their quantitative

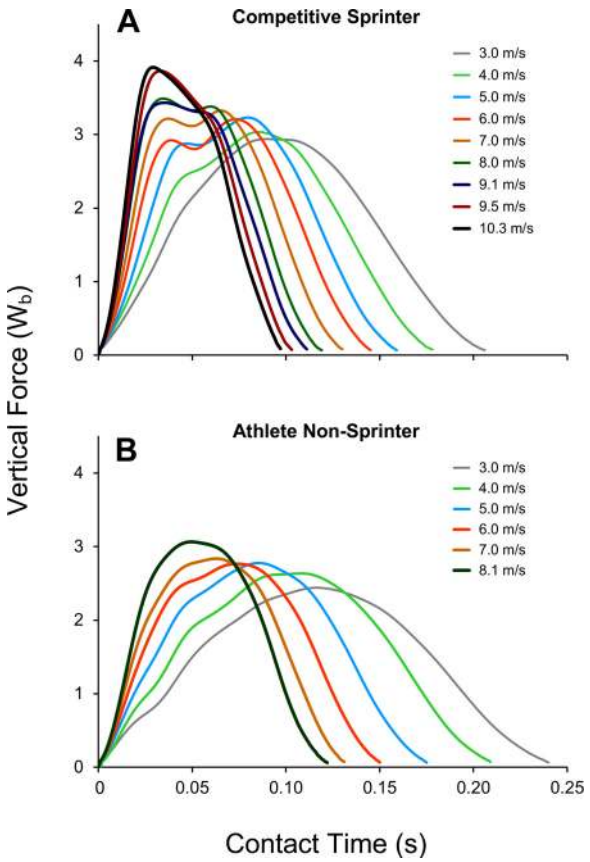

Fig. 4. Trial-averaged composite vertical ground reaction force-time waveforms across running speeds for the same female competitive sprinter (*A*) and female athlete nonsprinter (*B*) whose data appear in Figs. 2 and 3. For both subjects, stance-averaged vertical forces increased and ground contact times decreased across the range of speeds. (Confidence intervals are omitted for clarity, here and in subsequent figures).

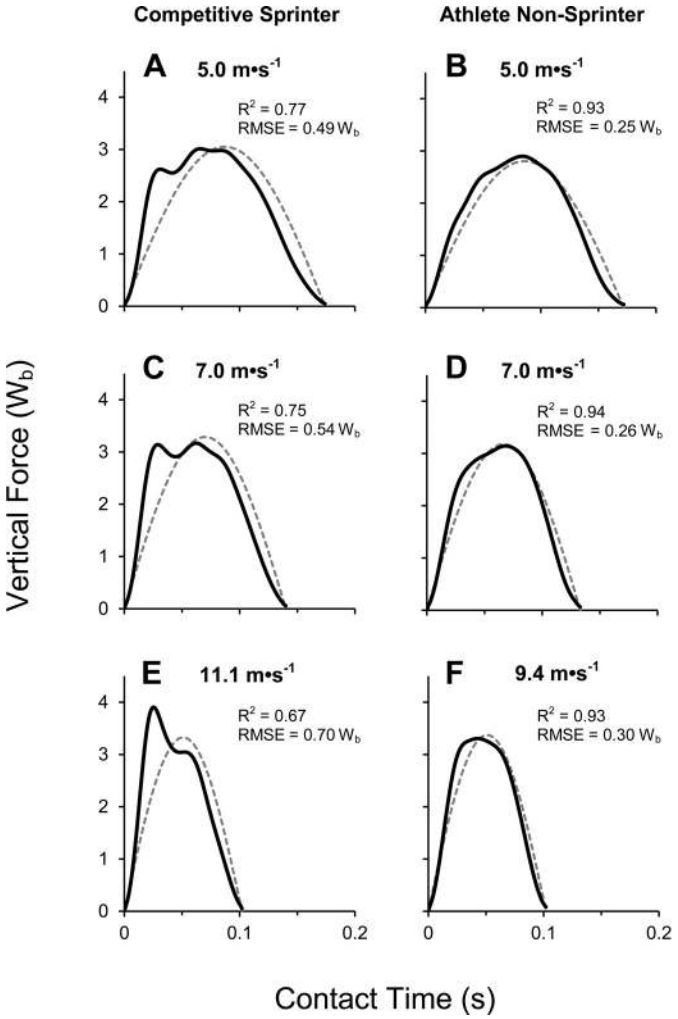

Fig. 5. The trial-averaged composite vertical ground reaction force-time waveforms for a representative male competitive sprinter and representative male athlete nonsprinter are plotted against the half-sine waveform predicted by the spring-mass model for 5.0 m/s, 7.0 m/s, and each individual's top speed (11.1 and 9.4 m/s for the competitive sprinter and athlete nonsprinter, respectively). The waveforms of the competitive sprinter progressively deviated from the spring-mass model as the speeds increased from 5.0 m/s to 7.0 m/s to top speed (*A*, *C*, and *E*), whereas the waveforms of the athlete nonsprinter generally conformed to the spring-mass model at all speeds (*B*, *D*, and *F*).

relationship to the spring-mass model predicted waveforms, appear in Fig. 5 for one male sprinter (Fig. 5, *A*, *C*, and *E*) and one male athlete nonsprinter (Fig. 5, *B*, *D*, and *F*). The male sprinter's waveforms have a qualitatively biphasic appearance due the rapid rising edge and early force peaks present on the waveforms at all three speeds. Thus patterns of ground force application for the sprinter were generally in relatively poor agreement with the spring-mass model at all three speeds (all R^2 values < 0.80). Because the rising edges of the waveforms were steeper and the early force peaks were greater in magnitude at faster speeds, the degree of conformation of the sprinters waveforms to the spring-mass model predicted waveforms decreased as speed increased, reaching an R^2 minimum of 0.67 at top speed. The ground reaction force waveforms of the male athlete nonsprinter lacked a rapid rising edge and conformed relatively closely to the spring-mass model at all three speeds (R^2 range: 0.93–0.94).

The ensemble-averaged waveform patterns of ground force application for the competitive sprint group and athlete nonsprint groups at the three test speeds (Fig. 6) exhibited the patterns similar to those of the individual athletes in Fig. 5, albeit to a slightly smaller degree. The rising edge of the group ensemble-averaged waveform for the competitive sprinters was steeper in general than that of the athlete nonsprinters, and became progressively more steep at the faster speeds. The group ensemble-averaged patterns of ground force application of the athlete nonsprinters conformed closely to the spring-model predicted waveforms at all three speeds (all R^2 values $\geq$ 0.93), exhibiting little discernible speed-related deviation.

The relative stance times at which the peak force occurred during top speed running, as assessed from the group composite waveforms in Fig. 6, *E* and *F*, were $t = 30.2\%$ of t_c for competitive sprinters and $t = 45.7\%$ of t_c for the athlete nonsprinters. The corresponding values for the percentage of

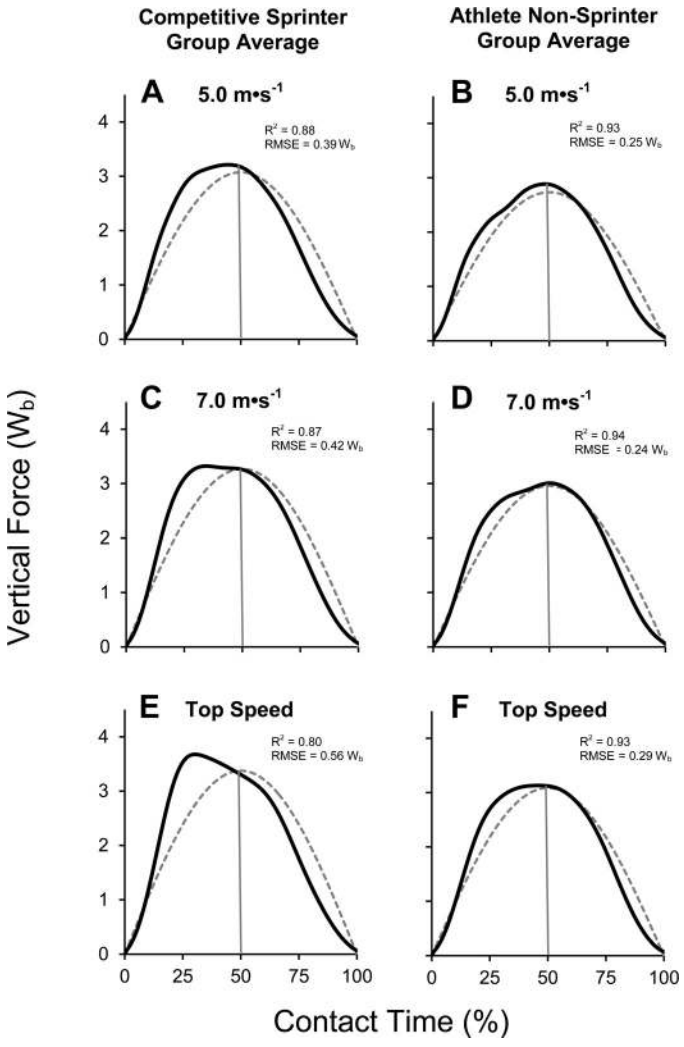

Fig. 6. The trial-averaged composite vertical ground reaction force-time waveform for the competitive sprinter group and the athlete nonsprinter group plotted against the half-sine waveform predicted by the spring-mass model for 5.0 m/s, 7.0 m/s, and top speed. The waveforms of the competitive sprinters progressively deviated from the spring-mass model predictions as the speed increased from 5.0 m/s to 7.0 m/s to top speed (*A*, *C*, and *E*), whereas the waveforms of the athlete nonsprinters generally conformed to the spring-mass model predictions at all speeds (*B*, *D*, and *F*).

the total contact time at which the center of mass reached its minimum height, as determined from the double-integration of the composite, top speed waveforms in Fig. 6, were $t = 40.5\%$ of t_c and $t = 48.7\%$ of t_c for the competitive sprinters and athlete nonsprinters, respectively.

Hypotheses One and Two: Statistical Test Results

The R^2 goodness of fit and RMSE force disagreement values (means ± SE) from the footfall waveforms ($n = 797$) analyzed at 5.0 m/s, 7.0 m/s, and top speed appear in Table 3. In keeping with our first hypothesis, the patterns of ground force application of the competitive sprinters conformed significantly less to the spring-mass model predictions than those of athlete nonsprinters when evaluated with the R^2 goodness of fit statistic (two-factor ANOVA, $F = 243.8$, $P < 0.001$). This was the case even when the much greater variability in the waveforms of the sprinters vs. athlete nonsprinters was taken into account by the Fligner-Killeen test. In partial support of our second hypothesis test using R^2 goodness of fit values, the patterns of ground force application conformed less to the simple spring-predicted pattern for sprinters at top speed than at 5.0 and 7.0 m/s. However, there were no significant differences across speed for athlete nonsprinters whose goodness of fit values were nearly identical at 5.0 m/s, 7.0 m/s, and top speed. Hence, interaction between athletic group and running speed was significant ($F = 51.5$, $P < 0.01$).

The hypothesis test results obtained when RMSE values were used to evaluate patterns of ground force application vs. those predicted by the spring-mass model were fully consistent with the results of the R^2 tests. The main effect of athletic group was significant, and there was an interaction between group and running speed. After again accounting for the lack of homogeneity of variance as tested by the Fligner-Killeen test, the RMSE force disagreement values vs. the simple-spring patterns predicted by the spring-mass model at all three test speeds were significantly greater for the competitive sprinters than the athlete nonsprinters ($F = 442.8$; df = 1, 795; $P < 0.001$). RMSE values were also statistically different across the three running speeds ($F = 104.0$; df = 5, 791; $P < 0.001$) with post hoc testing indicating that this difference was present for the competitive sprinters, but not the athlete, nonsprinters (Table 3).

Table 3. *Mean R^2 agreement and RMSE force disagreement values vs. the spring-mass model predicted waveforms*

Group	Steps, *n*	R^2	RMSE, W_b
Sprinter			
5.0 m/s	218	0.829 ± 0.007	0.440 ± 0.009
7.0 m/s	163	0.843 ± 0.008	0.437 ± 0.012
Top speed	67	0.782 ± 0.016*†	0.571 ± 0.025*†
Nonsprinter			
5.0 m/s	194	0.910 ± 0.003	0.276 ± 0.004
7.0 m/s	89	0.923 ± 0.004	0.276 ± 0.007
Top speed	66	0.915 ± 0.006	0.307 ± 0.012

RMSE, root mean square error. Competitive sprinters differed significantly from athlete nonsprinters across all speeds for both R^2 pattern agreement and RMSE force disagreement values (ANOVA, main effects, $P < 0.001$). Values are means ± SE. *Significantly different from 5.0 m/s; †significantly different from 7.0 m/s.

Individual Variability in Patterns of Ground Force Application

At each of the three analysis speeds, the standard errors about the R^2 and RMSE means were approximately two times greater for the sprinters than the athlete nonsprinters (Table 3). The greatest within-group stratification for both variables existed among the four men in the competitive sprinter group. For the ensemble-averaged waveforms, *subjects 1* and *2* had respective R^2 goodness of fit values to the spring-mass model predicted waveforms of 0.78 and 0.73 across the three test speeds, whereas *subjects* 3 and *4* had respective values of 0.89 and 0.91. The corresponding RMSE values for *subjects 1* and *2* were 0.62 and 0.58 W_b, respectively, vs. 0.35 and 0.37 W_b for *subjects 3* and *4*. Top speed patterns of ground force application for these respective pairs of competitive male sprinters (*subjects 1* and *2*, elite vs. *subjects 3* and *4*, sub-elite) and the corresponding ensemble average of all of the male subjects in the athlete nonsprinter group ($n = 4$) appear in Fig. 7*A*. The trend most evident for male sprinters was present throughout the entire sample. Differences in the stance-average vertical forces applied at top speed were determined entirely during the first half of the stance period (Fig. 7*B*) because all 14 subjects in our sample applied nearly the same vertical force over the second half of the stance phase (1.72 ± 0.04 W_b).

DISCUSSION

Our first objective was to answer the basic question posed in our title: are running speeds maximized with simple-spring stance mechanics? Although selected results did not precisely conform to our predictions, our data in total provided a definitively negative answer. With nearly complete consistency, we found that the runners who applied the greatest mass-specific vertical forces, and thereby attained the fastest speeds, deviated most from the simple-spring pattern of ground force application predicted by the spring-mass model (Figs. 2, 4, 5, 6, and 7; Table 3). Given the need for all runners to reduce periods of ground force application as they run faster, these data provide two closely linked conclusions. First, the simple-spring patterns of ground force application generally regarded as advantageous at slower speeds (15, 16, 31) likely constrain force application and performance at faster ones. Second, deviating from simple-spring, stance mechanics appears to be a strategy that sprinters use (14) to apply the greater mass-specific ground forces needed to attain faster speeds.

Hypothesis Test Outcomes: Simple-Spring Stance Mechanics at the Fastest Speeds?

From a strictly experimental perspective, our first simple-spring hypothesis test outcome conformed to our expectations in full, whereas our second outcome conformed only in part. As predicted, *test 1*, which used athletic specialization as an experimental tool, revealed that the patterns of ground force application of the competitive sprinters deviated more from simple-spring predicted behavior than those of athlete nonsprinters regardless of speed (Table 3). Between-group quantitative differences were sufficiently large to be qualitatively obvious from the shapes of the waveforms, whether for individual athletes (Figs. 4 and 5), or the entire athletic specialty groups (Figs. 6 and 7). However, *test 2*, which used across-

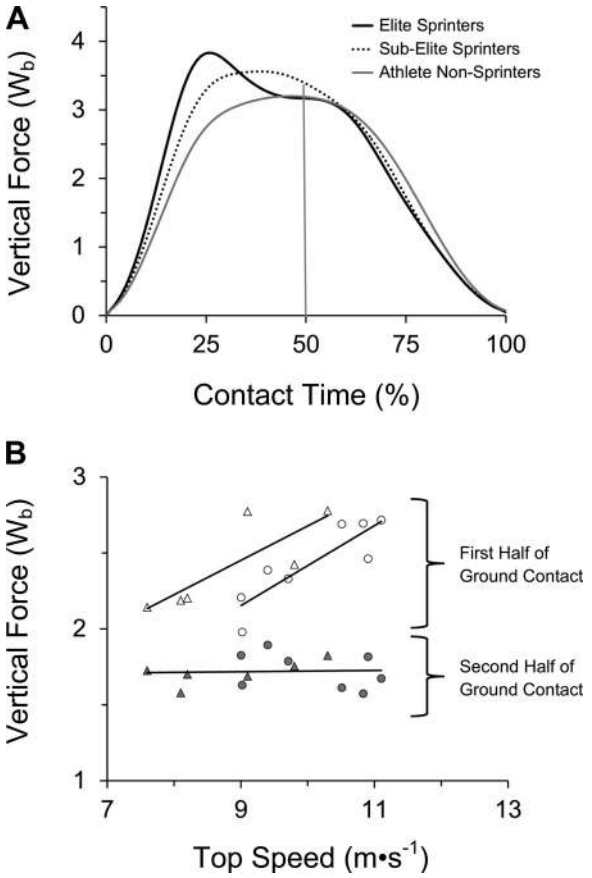

Fig. 7. Trial-averaged composite vertical ground reaction force-time waveforms vs. top speed for the two male elite sprinters (solid black line), the two male sub-elite sprinters (dotted black line), and four male athlete nonsprinters (solid gray line) (*A*). Average vertical forces for the first and second half of the ground contact period for subjects in both groups at top speed (*B*). Circles represent male subjects; triangles represent females subjects; open symbols represent average vertical forces for the first half of the ground contact; shaded symbols represent average vertical forces for the second half of ground contact period. Line fits for the data from the first half of the ground contact period are provided by sex to appropriately account for the leg and contact length differences (Eq. 5, Table 2) that influence top speeds. A single line fit for the data from the second half of the ground contact period is plotted for all 14 subjects because the values are similar in magnitude across group and sex. [Linear best-fit regression equations appearing in *B* that relate ground force to top running speeds are as follows: men first half-stance, force (W_b) = 0.26·Spd − 0.22; women first half contact, force (W_b) = 0.23·Spd + 0.41; all subjects second half contact force (W_b) = 0.004·Spd + 1.68].

speed comparisons as an experimental tool, yielded results that were mixed by athletic specialization; differences across speed were present for the competitive sprinters, but absent for the athlete nonsprinters. For the competitive sprinters, R^2 pattern-agreement and RMSE force-disagreement values at 5.0 and 7.0 m/s were similar to one another (R^2 range 0.83 to 0.85; RMSE range 0.43 to 0.44 W_b; Table 3), whereas their top-speed patterns deviated significantly more from model predictions (R^2 <0.80; RMSE >0.55 W_b). Using our R^2 threshold of 0.90 for simple-spring vs. nonsimple-spring patterns, the sprinters did not conform to simple-spring predictions at any of the three speeds, and deviated most at top speed. In contrast, the athlete nonsprinters used patterns of ground force application that conformed relatively closely (R^2 >0.90) regardless of whether they were running at top speed or the two fixed test speeds of 5.0 and 7.0 m/s (Table 3). Unlike the competitive sprinters, the athlete nonsprinters exhibited virtually no differences in their patterns of ground force application across speed. Both their R^2 pattern-agreement and RMSE force-disagreement values vs. the model predicted patterns model were essentially identical across 5.0 m/s, 7.0 m/s, and top speed (ΔR^2 <0.02; ΔRMSE = 0.03 W_b).

Although our results across running speed were mixed with respect to our hypothesis, the conclusions regarding the force application patterns that maximize running speed were fully consistent. The across-speed results obtained from the competitive sprinters suggest that deviating from a simple-spring pattern of ground force application may be a mechanism these athletes used to attain faster speeds. Athlete nonsprinters, in contrast, did not alter their patterns across speed, nor deviate appreciably from simple-spring pattern at any speed. Notably, we found essentially the same pattern contrasts across individual subjects of differing performance capabilities. Of the four men in the competitive sprinter group, the two nonelite athletes (*subjects 3* and *4*) used top-speed, stance-limb mechanics reflective of their intermediate performance status. Specifically, these two sub-elite men had stance-limb mechanics that deviated more from the simple-spring predicted pattern than the athlete nonsprinters whom they could outperform. However, their mechanics deviated less from the pattern (R^2 means of 0.83 vs. 0.71, respectively) than those of the two world-class men (Fig. 7*A*, Table 3). Collectively, these observations suggest that the deviation from the simple-spring pattern observed for the world-class sprinters may be a force-augmentation mechanism that sub-elite sprinters cannot utilize to the same degree, and that athlete nonsprinters may be generally unable to use at all.

Applicability of the Spring-Mass Model to High-Speed Running

The broad acceptance of the spring-mass model over the course of the last two decades has been heavily based on running and hopping data from relatively slow speeds (4, 18, 19, 26, 33). The more recent application of the model to faster running speeds (25, 27, 34) is understandable given positive results from slower speeds and the limited data available at faster ones (6). The data set we have compiled here includes hundreds of high-speed running footfalls from athletes spanning a broad range of sprinting abilities. The emergent finding from these data that the fastest speeds are achieved via consistent, specific deviation from the model's predictions warrants critical evaluation of the spring-mass model's assumed applicability to sprint running.

One means of assessing relative conformation to the spring-mass model is to examine the model-predicted force-motion dynamics vs. those actually observed. The model predicts that the peak force will occur at the temporal midpoint of the foot-ground contact period (i.e., at t = 50% of t_c), and that the center of mass will reach its lowest position at the same time. We found that our athlete nonsprinters conformed to these model-predicted behaviors somewhat (Fig. 6*F*), whereas our competitive sprint subjects conformed little or not at all. For the competitive sprinters at top speed, the group-averaged, ensemble waveform exhibited a force peak at t = 30% of t_c (Fig. 6*E*), and a corresponding height minimum of the center of

mass at $t = 40\%$ of t_c rather than the model-predicted values of $t = 50\%$ for both. Many of the individual sprinter's waveforms at faster speeds had force peaks that occurred at $t \leq 25\%$ of t_c (Figs. 2*A*, 4*A*, 5*E*), and some exhibited two force peaks, with the first occurring at $t \approx 20\%$ and the second at $t \approx 50\%$ of t_c (Fig. 5*C*). By even generous assessment, these results indicate that the spring-mass model is a poor descriptor of the stance-limb mechanics of high-caliber sprint athletes. These findings also raise basic questions about using the vertical and limb stiffness variables derived from the spring-mass model to describe the mechanics of running at higher speeds (25, 27, 34). The value of these stiffness variables as descriptors of sprint running mechanics is at best unclear if sprinting performance is optimized by not conforming to the assumptions required to calculate them.

The prior success of the spring-mass model as a descriptor of running mechanics raises an immediate question regarding our negative test outcomes for sprinters: why do these athletes not conform to the model when so many other runners and hoppers do? Our results suggest that the performance demands of sprinting are probably not compatible with the stance-limb mechanics predicted by the simple, linear spring in the spring-mass model. The model was formulated as a mechanical approximation for describing the apparently spring-like center of mass dynamics observed in the early, classic studies on gait mechanics (4, 11, 26). The presence of spring-like mechanics that the original investigators inferred at the level of the whole limb have subsequently been measured in selected muscles, tendons, and ligaments that contribute to the limb's overall behavior (21, 30). Indeed, during slower-speed running and hopping, the tissue-level stretch-shortening cycles (21, 31) that conserve mechanical energy could contribute as theorized to waveform patterns that generally conform to the predictions of the spring-mass model at these speeds (8). However, as considered in detail elsewhere (10), the success of sprinters does not depend upon either the conservation of mechanical energy or locomotor economy, but rather upon the ability to apply large mass-specific forces to the ground quickly.

An important caution is warranted in the interpretation of our finding that the mechanics of the fastest human runners generally do not conform to the predictions of the spring-mass model. Specifically, the deviations we report from the simple, linear-spring predicted behavior of the model should not be interpreted more broadly as an absence of either spring-like dynamics or energy storage. Indeed, the greater ground reaction forces observed in faster runners and at faster speeds may coincide with relatively greater tissue strains and energy storage (21, 31). Rather, our findings are best understood within the context of our test objectives and the limitations of the classic spring-mass model. Our objectives required a null standard of comparison for the purpose of quantifying different patterns of ground force application. We used the simple, linear-spring predictions of the spring-mass model for this purpose because these waveforms have served as the literature standard for well over a decade. However, our objectives could have been just as easily met by using some other pattern as a standard of comparison. Accordingly, we caution against interpreting the patterns reported using an energy storage framework.

Ground Force Application Strategies for Speed

Swifter runners are known to attain their faster top speeds primarily by applying greater mass-specific forces to the ground, but the mechanism by which they do so has not been previously identified. Here, two design strategies helped us to elucidate the force application strategy they use. First, we chose to analyze force application on a millisecond-by-millisecond basis rather than by averaging over the full stance period (per Fig. 3) as previously (36–38). Second, we recruited a pool of athletic subjects with a fairly broad range of individual top speeds. The latter strategy included enrolling four sprinters who were world-class track athletes (Table 1, *subjects 1*, *2*, *5*, and *6*) and a fifth who was a national-class athlete with Olympic and world championship experience (*subject 7*). The scores of sprint-running force waveforms acquired from this heterogeneous group of fast-running athletes provided force and speed data not previously available from this population. The consistent manner in which faster runners deviated from the pattern predicted by the simple spring-mass model to apply greater mass-specific forces provided crucial mechanistic insight.

Our finding that speed is maximized via a common force application strategy was certainly not a foregone conclusion at the outset of the study. From a purely theoretical perspective, the data acquired might have resulted in several outcomes other than the one we obtained. For example, faster athletes might have applied greater forces while utilizing a simple, linear-spring pattern. Alternatively, they might have employed an asymmetrical strategy that resulted in the greatest forces occurring later rather than earlier in the stance period. Finally, different athletes might have used different patterns to maximize force application and speed. Our finding that the degree of conformation to a particular pattern was consistently related to magnitude of the mass-specific force applied and top speeds attained provides two basic conclusions. First, our data indicate that the fastest human runners have converged on a common mechanical solution for maximizing ground force and speed. Second, the convergence on a common solution implies the existence of a single most effective mechanism by which human runners can maximize speed.

Indeed, the mechanical strategy identified was so consistent that even simple approaches to examining stance-phase patterns of force application were sufficient to reveal it. When the top speed forces of our 14 subjects were assessed by dividing the stance period into halves (Fig. 7*B*), this simple analysis revealed that individual differences in the total stance-averaged forces were all but completely determined during only one of the two periods. Specifically, we found a strong positive relationship between top speed and the average force applied during the first half of the stance period, and essentially no relationship to the average force applied during the second half. These respective results are illustrated in Fig. 7*B*, with the first-half, best-fit relationships being provided by sex to appropriately account for the leg and contact length differences (Equation 5, Table 2) that directly influence top speeds.

An immediate question raised by our findings is why essentially all of the differences in stance-averaged forces at top speed are attributable to a relatively small portion of the total stance period. We cannot fully answer this question on the basis of force application data alone. However, the

results illustrated in Fig. 7 and those from our Fourier analysis (see APPENDIX) are consistent with the impact-phase, limb-deceleration mechanism we have recently described (14). This mechanism appears to explain how several of the gait features classically associated with competitive sprinters (24) translate into the greater mass-specific ground forces they apply. First, the knee elevation sprinters achieve late in the swing phase appears to contribute to early stance ground force application by allowing greater limb velocities to be achieved prior to foot-ground impact (24). Second, the erect stance-phase posture sprinters adopt likely contributes to the stiffness required to decelerate the limb and body relatively quickly after the instant of foot-ground impact. The progressive, rising-edge deviation observed vs. the simple spring pattern, in relation to both top sprinting speeds (Figs. 5, 6, and 7) and across different speeds in individual sprinters (Figs. 2*A*, 5*A*, 5*C*, 5*E*, 6*A*, 6*C*, 6*E*, and 7) is consistent with the impact-phase, limb deceleration differences that may present across these trials (14).

Concluding Remarks: A Ground Force Signature for Speed

We conclude that a relatively specific, asymmetrical pattern of force application maximizes the ground forces runners can apply during the brief contact periods that sprinting requires. The factors responsible for the pattern are not yet fully known, but result in the fastest sprinters applying substantially greater forces than nonsprinters during the early portion of the stance period. Consistent pattern asymmetry among the swiftest sprinters, and less pronounced pattern asymmetry among less-swift athletes lead us to conclude that *1*) the fastest athletes have converged on a common mechanical solution for speed, and *2*) that less-swift athletes generally do not execute the pattern. On this basis, we suggest that the force-time pattern documented here for the most competitive sprinters in our sample (Fig. 7*A*; supplementary video) constitutes a ground force application signature for maximizing human running speeds.

APPENDIX

Vertical ground reaction force waveforms during running are composed of high-frequency components due to the acceleration of the lower limb during the impact phase, and low-frequency components due to the acceleration of the rest of the body during the entire contact phase (14). Fourier analysis can be used to analyze these components.

Any time-varying signal *s(t)* can be represented as a sum of sine waves [(39), Equation 2.3, p. 28] and can be expressed as:

Table A1. *Fourier terms of competitive sprinter at 11.1 m/s measured force data*

Harmonic	f_n, Hz	a_n, W_b	θ_n, Radians
0		2.1739	
1	9.8039	1.5513	−0.9871
2	19.6078	0.6461	−1.2683
3	29.4118	−0.3049	0.6676
4	39.2157	−0.0678	0.0262

f_n, Frequency of the harmonic; a_n, amplitude of the harmonic; θ_n, phase of the harmonic.

Table A2. *Fourier terms of competitive sprinter at 11.1 m/s modeled half-sine waveform*

Harmonic	f_n, Hz	a_n, W_b	θ_n, Radians
0		2.1739	–
1	9.8039	1.4664	−1.5721
2	19.6078	0.2968	−1.5733
3	29.4118	−0.1297	1.5672
4	39.2157	0.0740	−1.5755

Table A3. *Fourier terms of athlete nonsprinter at 9.4 m/s measured force data*

Harmonic	f_n Hz	a_n, W_b	θ_n, Radians
0		2.1199	
1	9.8039	1.5324	−1.3331
2	19.6078	0.4448	−1.4240
3	29.4118	−0.1038	0.8629
4	39.2157	−0.0382	0.4151

Table A4. *Fourier terms of athlete nonsprinter at 9.4 m/s modeled half-sine waveform*

Harmonic	f_n, Hz	a_n, W_b	θ_n, Radians
0		2.1199	
1	9.8039	1.4299	−1.5721
2	19.6078	0.2895	−1.5733
3	29.4118	−0.1265	1.5672
4	39.2157	0.0722	−1.5755

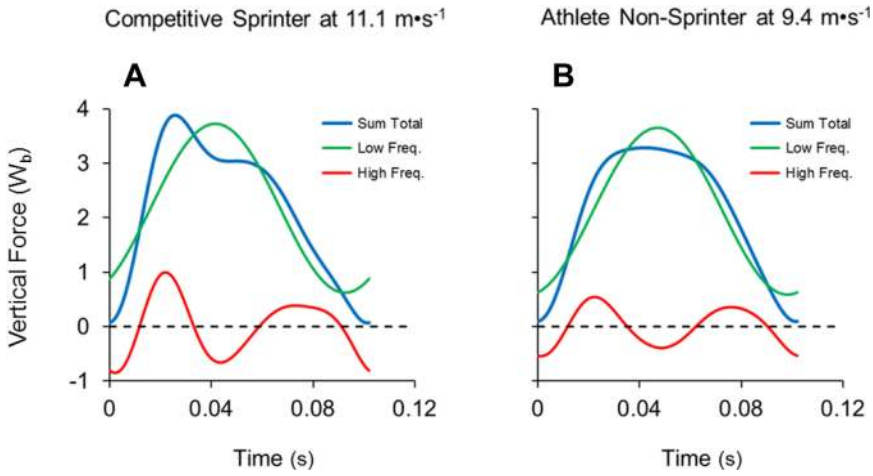

Fig. A1. These graphs are generated from the Fourier terms listed in Table A1 (competitive sprinter at 11.1 m/s) (*A*) and Table A3 (athlete nonsprinter at 9.4 m/s) (*B*). Low-frequency components (green line) include terms $n = 0$ and $n = 1$; high-frequency components (red line) include terms $n = 2$, $n = 3$, and $n = 4$. The summation of all components (blue line) accurately reproduces the original measured data.

$$s(t) = a_0 + \sum_{n=1}^{N} a_n \sin\left(2\pi f_n t + \theta_n\right) \qquad (Eq.\ 6)$$

where a_o is the mean of the signal, and f_n, a_n, and θ_n are the frequency, amplitude, and phase angle of the nth harmonic, respectively. The signal or waveform can be reproduced from these variables using N harmonics, with reproductive accuracy increasing as N increases.

To serve as an example of performing the Fourier analysis, the measured force data and modeled half-sine waveforms from Fig. 5, *E* and *F*, were analyzed using Equation 6. For both the competitive sprinter and the athlete nonsprinter, the trial average contact time was 0.102 s. The force data were measured on an instrumented force treadmill and filtered at 25 Hz. Four harmonics ($n = 4$) were sufficient to accurately reproduce the original measured data and the modeled half-sine waveforms.

Tables A1–A4 provide the terms for the variables described in Equation 6. The waveforms appearing in Fig. A1, *A* and *B*, were generated from the terms listed in Table A1 and Table A3, respectively. Low-frequency components (green line) include terms $n = 0$ and $n = 1$ and high-frequency components (red line) include terms $n = 2$, $n = 3$, and $n = 4$. The summation of all components (blue line) accurately reproduces the measured data.

The appearance of waveform differences above, but not below, the 10 Hz domain, is consistent with the time course of the impact-phase, force-enhancement mechanism proposed recently (14) and included here to explain the differences observed between the patterns of ground force of competitive sprinters vs. athlete, nonsprinters.

ACKNOWLEDGMENTS

We thank Dr. L. Ryan for assistance with data collection, instrumentation, technical support, manuscript critique, and substantial contributions to the scientific analysis; Dr. K. Roberts for contributions to the statistical analysis; Coach A. Behm and Dr. Robert Chapman for strategic guidance and support; and the 14 athletes who made the study possible by volunteering their time and effort.

GRANTS

Support for this study was provided in part by U.S. Army Medical and Materiel Command Award 17-02-2–0053 to P.G.W., and by funding from Southern Methodist University's Simmons School of Education and Human Development to K.P.C.

DISCLOSURES

No conflicts of interest, financial or otherwise, are declared by the author(s).

AUTHOR CONTRIBUTIONS

Author contributions: K.P.C. and P.G.W. conception and design of research; K.P.C. and P.G.W. performed experiments; K.P.C. and P.G.W. analyzed data; K.P.C. and P.G.W. interpreted results of experiments; K.P.C. and P.G.W. prepared figures; K.P.C. and P.G.W. drafted manuscript; K.P.C. and P.G.W. edited and revised manuscript; K.P.C. and P.G.W. approved final version of manuscript.

REFERENCES

1. **Alexander RM, Jayes AS.** Fourier analysis of the forces exerted in walking and running. *J Biomech* 13: 383–390, 1980.
2. **Alexander RM, Maloiy GM, Hunter B, Jayes AS, Nturibi J.** Mechanical stresses during fast locomotion of buffalo *(Syncerus caffer)* and elephant *(Loxodonta africana)*. *J Zool Lond* 189: 135–144, 1979.
3. **Bezodis IN, Kerwin DG, Salo AI.** Lower-limb mechanics during the support phase of maximum-velocity sprint running. *Med Sci Sports Exerc* 40: 707–715, 2008.
4. **Blickhan R.** The spring-mass model for running and hopping. *J Biomech* 22: 1217–1227, 1989.
5. **Bruggeman GP, Arampatzis A, Emrich F, Potthast W.** Biomechanics of double transtibial amputee sprinting using dedicated sprint prostheses. *Sports Technol* 1: 220–227, 2009.
6. **Brughelli M, Cronin J.** A review of the literature on the mechanical stiffness in running and jumping: methodology and implications. *Scand J Sport Med* 18: 417–426, 2008.
7. **Bullimore SR, Burn JF.** Consequences of forward translation of the point of force application for the mechanics of running. *J Theor Biol* 238: 211–219, 2006.
8. **Bullimore SR, Burn JF.** Ability of the planar spring-mass model to predict mechanical parameters in running humans. *J Theor Biol* 248: 686–695, 2007.
9. **Bundle MW, Hoyt RW, Weyand PG.** High speed running performance: a new approach to assessment and prediction. *J Appl Physiol* 95: 1955–1962, 2003.
10. **Bundle MW, Weyand PG.** Sprint exercise performance: does metabolic power matter? *Exerc Sport Sci Rev* 40: 174–182, 2012.
11. **Cavagna GA, Sabiene FP, Margaria R.** Mechanical work in running. *J Appl Physiol* 19: 249–256, 1964.
12. **Cavagna GA.** Force platforms as ergometers. *J Appl Physiol* 39: 174–179, 1975.
13. **Cavagna GA, Heglund NC, Taylor CR.** Two basic mechanisms for minimizing energy expenditure. *Am J Physiol Regul Integr Comp Physiol* 233: R243–R261, 1977.
14. **Clark KP, Ryan LJ, Weyand PG.** Foot speed, foot-strike and footwear: linking gait mechanics and running ground reaction forces. *J Exp Biol* 217: 2037–2040, 2014.
15. **Dalleau G, Belli A, Bourdin M, Lacour JR.** The spring-mass model and the energy cost of treadmill running. *Eur J Appl Physiol* 77: 257–263, 1998.
16. **Dickinson MH, Farley CT, Full RJ, Koehl MA, Kram R, Lehman S.** How animals move: an integrated view. *Science* 288: 100–106, 2000.
17. **Farley CT, Blickhan R, Saiot J, Taylor CR.** Hopping frequency in humans: a test of how springs set stride frequency in bouncing gaits. *J Appl Physiol* 71: 2127–2132, 1991.
18. **Farley CT, Gonzalez O.** Leg stiffness and stride frequency in human running. *J Biomech* 29: 181–186, 1996.
19. **Farley CT, Houdijk HH, Van Strien C, Louie M.** Mechanism of leg stiffness adjustment for hopping on surfaces of different stiffnesses. *J Appl Physiol* 85: 1044–1055, 1998.
20. **Frishberg BA.** An analysis of overground and treadmill sprinting. *Med Sci Sports Exerc* 15: 478–485, 1983.
21. **Ker RF, Bennett MB, Bibby SR, Kester RC, Alexander RM.** The spring in the arch of the human foot. *Nature* 325: 147–149, 1987.
22. **Kram R, Griffin TM, Donelan JM, Chang YH.** Force treadmill for measuring vertical and horizontal ground reaction forces. *J Appl Physiol* 85: 764–769, 1998.
23. **Kuitunen S, Komi PV, Kyröläinen H.** Knee and ankle joint stiffness in sprint running. *Med Sci Sports Exerc* 34: 166–173, 2002.
24. **Mann RV.** The mechanics of sprinting and hurdling. *CreateSpace* 2011.
25. **McGowan CP, Grabowski AM, McDermott WJ, Herr HM, Kram R.** Leg stiffness of sprinters using running-specific prostheses. *J R Soc Interface* 9: 1975–82, 2012.
26. **McMahon TA, Cheng GC.** The mechanics of running: how does stiffness couple with speed? *J Biomech* 23, *Suppl* 1: 65–78, 1990.
27. **Morin JB, Dalleau G, Kyröläinen H, Jeannin T, Belli A.** A simple method for measuring stiffness during running. *J Appl Biomech* 21: 167–180, 2005.
28. **Munro CF, Miller DI, Fuglevand AJ.** Ground reaction forces in running: a reexamination. *J Biomech* 20: 147–155, 1987.
29. **Riley PO, Dicharry J, Franz J, Della Croce U, Wilder RP, Kerrigan DC.** A kinematics and kinetic comparison of overground and treadmill running. *Med Sci Sports Exerc* 40: 1093–1100, 2008.
30. **Roberts TJ, Marsh RL, Weyand PG, Taylor CR.** Muscular force in running turkeys: the economy of minimizing work. *Science* 275: 1113–1115, 1997.
31. **Roberts TJ, Azizi E.** Flexible mechanisms: the diverse roles of biological springs in vertebrate movement. *J Exp Biol* 214: 353–361, 2011.
32. **Robilliard JJ, Wilson AM.** Prediction of kinetics and kinematics of running animals using an analytical approximation to the planar spring-mass system. *J Exp Biol* 208: 4377–4389, 2005.
33. **Srinivasan M, Holmes P.** How well can spring-mass-like telescoping leg models fit multi-pedal sagittal-plane locomotion data? *J Theor Biol* 255: 1–7, 2008.

34. **Taylor MJ, Beneke R.** Spring-mass characteristics of the fastest men on earth. *Int J Sports Med* 33: 667–670, 2012.
35. **Usherwood JR, Hubel TY.** Energetically optimal running requires torques about the centre of mass. *J R Soc Interface* 9: 2011–5, 2012.
36. **Weyand PG, Sternlight DB, Bellizzi MJ, Wright S.** Faster top running speeds are achieved with greater ground forces not more rapid leg movements. *J Appl Physiol* 81: 1991–1999, 2000.
37. **Weyand PG, Bundle MW, McGowan CP, Grabowski A, Brown MB, Kram R, Herr H.** The fastest runner on artificial limbs: different limbs, similar function? *J Appl Physiol* 107: 903–911, 2009.
38. **Weyand PG, Sandell RF, Prime DN, Bundle MW.** The biological limits to running speed are imposed from the ground up. *J Appl Physiol* 108: 950–961, 2010.
39. **Winter DA.** Biomechanics and motor control of human movement (2nd ed.). New York, NY: John Wiley and Sons, 1990.